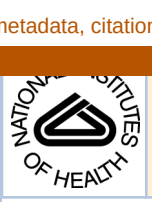

Published in final edited form as:

Small. 2012 June 25; 8(12): 1876–1879. doi:10.1002/smll.201102418.

Microfluidic generation of acoustically active nanodroplets **

Thomas D. Martz[1], **David Bardin**[2], **Paul S. Sheeran**[3], **Abraham P. Lee**[2], and **Paul A. Dayton**[3,*]

[1]Curriculum of Applied Science & Engineering - Material Science, University of North Carolina-North Carolina State University, Chapel Hill, NC, USA

[2]Department of Biomedical Engineering, University of California-Irvine, Irvine, California, USA

[3]Joint Dept. of Biomedical Engineering, University of North Carolina-North Carolina State University, Chapel Hill, NC, USA

Liquid perfluorocarbon (PFC) droplets have emerged in medical acoustics as acoustically activatable emulsions for a variety of applications. The phase-shift of the inner core of a perfluorocarbon droplet from the liquid state to the gas state as a result of an applied ultrasound pressure is most commonly referred to as acoustic droplet vaporization (ADV).[1] While most ADV investigations have focused on droplets in the micron range for intravascular procedures, there has been much recent interest in the utility of sub-micron liquid perfluorocarbon droplets for extravascular applications such as drug delivery, enhanced thermal ablation, and diagnostic imaging and tissue characterization.[2,3] Capitalizing on the characteristically 'leaky' vasculature of many solid tumors, sub-micron droplets may extravasate into the tumor interstitium through inter-endothelial gaps and accumulate[4], or may be able to traverse the lymphatic system. One main limitation of current methods to generate these nanodroplets is the use of processing techniques such as emulsification[5] and sonication[6], which result in polydisperse populations. Significant variation is reported in the activation threshold due to the strong correlation between vaporization energy and perfluorocarbon droplet size.[7,8] Additionally, the biodistribution of sub-micron ADV agents may improve by narrowing the size distribution. Substantial clinical motivation thus exists for a precise method to generate perfluorocarbon nanodroplets for use in extravascular tumor therapies. The emergence of droplet-based microfluidic systems has enabled the generation of droplets in the micrometer diameter range with high uniformity[9,10]; yet, the generation of nanodroplets from devices with microscale geometry still presents a fundamental challenge. Previous microfluidic approaches to produce nanodroplets have relied on the inherently inefficient dynamic sorting of small satellite droplets (as small as 100 nm) from microscale droplet populations as the basis of a monodisperse submicron emulsification system.[10,11,12] To overcome this limitation, we hypothesized that by modulating the basic mechanism of droplet generation to access a more favorable droplet formation regime[13,14,15], we could yield an efficient approach for the generation of perfluorocarbon nanodroplets as the primary emulsion.

Our group recently demonstrated the feasibility of microfluidic generation of microscale ADV agents to achieve precision control of droplet size and uniform activation.[7, 15] In this study, we advance upon this prior work with the development of a microfluidic system capable of generating populations of primary *sub-micron* droplets with diameters as small as 300–400 nm through two key refinements of the previously explored systems. In the earliest

*Corresponding Author: Prof. Paul A. Dayton, Thomas D. Martz, and Paul S. Sheeran, 304 Taylor Hall, CB 7575, Chapel Hill, NC 27599 (USA), padayton@bme.unc.edu.
David Bardin and Prof. Abraham Lee, 3406 Engineering Hall, Irvine, CA, 92697, (USA)

study, syringe pumps were used to control input rates of all reagents, but the mechanical variability inherent to syringe-pump driven systems[16] led to a lower limit of approximately 7 μm in diameter.[7] By controlling the dispersed perfluoropentane phase with a custom pressure-controlled input similar to that used in prior studies[16, 17], droplet sizes were reduced to 3–5 μm.[15] Here, we demonstrate that pressure-controlled delivery of all reagents (Figure 1a) affords the ability to drive the microfluidic device into a tip-streaming regime[18] with extremely low variability – enabling sub-micron droplet production despite the fact that the orifice width is over an order of magnitude larger than the droplets themselves (Figure 1b). We also observed that increasing the viscosity of the continuous phase through the addition of glycerol greatly enhanced the ability to drive droplet production stably in the sub-micron regime at the high pressures used. Relative to satellite droplet sorting, advanced tip-streaming, as we demonstrate, allows for efficiency in generating droplets in the sub-micron range, without filtration or dynamic in-device separation.

By precisely varying the pressures and, consequently, the flow rates of the continuous and dispersed phases, we were able to produce narrowly dispersed lipid-encapsulated nano- and microdroplets ranging from 360 nm to 11 μm with the same microfluidic device (Table 1). Although some variability was observed between devices generated from the same mask, droplets between 3 μm and 11 μm were achieved by driving the dispersed phase with 12–15 psi with the continuous phase at 33–35 psi. Droplets on the order of 800–900 nm were achieved by driving the dispersed phase with 16–17 psi with the continuous phase kept near 44–45 psi. By driving the dispersed phase with a pressure of 19–20 psi while the continuous phase was kept at 50 psi, droplets on the order of 300–400 nm were produced. Channel "blowouts" were observed when pressures on the order of 60 psi were used to drive reagent flow.

Droplets larger than 1 μm were quantified with high-speed light microscopy as they exited the orifice. Smaller droplets could not be resolved with traditional light microscopy, and hence were collected and then assessed by dynamic light scattering (DLS) with a Malvern Nanosizer (Figure 2) after production (thus, production rate data was not obtained for these flow conditions). Transmission electron microscopy (TEM) of a number of the samples were used to verify DLS results (Figure 3). The average diameter measured by TEM over 30 droplets was 312 ± 49 nm, which is in excellent agreement with the DLS measurements for the same sample (Figure 2, Sample 1). One of the consequences of using a lipid-based continuous phase in conjunction with microfluidics is a high degree of naturally-occurring lipid vesicles, typically on the order of 100 nm or less. In these experiments, the presence of lipid vesicles was confirmed by both DLS and TEM, appearing as peaks on the order of 30 – 70 nm in DLS measurements (Figure 2), and resulting in a heterogeneous background in TEM images composed of a high number of clearly visible non-PFC particles below 100 nm in size (Figure 3).

In order to confirm the resulting samples were acoustically vaporizable, droplets were sonicated with 100-cycle pulses of varying amplitude at 3.2 MHz. As described previously[7,8,19], the pressure required to vaporize droplets increases as droplet size decreases. In this study, a peak rarefactional pressure of approximately 3.15 MPa was sufficient to vaporize the majority of droplets in focus when the droplet size was greater than approximately 7 μm in diameter. As expected, smaller samples required substantially more pressure to vaporize. Droplets near 0.9 μm in diameter required approximately 4 MPa to vaporize, while smaller droplets could not be vaporized due to the maximum output limit of our ultrasound system (4.3 MPa). Activation thresholds established from this study are in agreement with thresholds previously identified for individual perfluoropentane droplets.[7]

Our results demonstrate that sub-micron (and micron) droplets for acoustic droplet vaporization applications can be effectively generated using droplet-based microfluidics. The pressure-controlled reagent delivery system crucially enabled the quick and precise tuning of the continuous and dispersed phases to maintain constant rates of flow and consistent tip-streaming. By contrast, in our prior studies utilizing mechanical pumping, we were unable to maintain the tip-streaming of sub-micron droplets for sufficient time to collect samples. To our knowledge, this study is one of the first examples of sub-micron production of primary liquid droplets from a microfluidic device. Future studies are needed to determine the extent that similarly small droplets can be produced with reagents other than those used here. The ability to achieve sub-micron droplet production, as well as the ability to produce droplet populations of uniform size, will have a significant impact in burgeoning medical applications requiring acoustically active nano- and microdroplets.

Experimental Section

Reagent Preparation

The continuous phase lipid solution was prepared using a 9:1 molar ratio of 1,2-distearoyl-sn-glycero-3-phosphocoline (DSPC) (Avanti Polar Lipids, Alabaster, AL) and 1,2-distearoyl-sn-glycero-3-phosphoethanolamine-N[methoxy-(polyethylene glycol)-5000] (DSPE-PEG5000) (Avanti Polar Lipids, Alabaster, AL) in saline (lipid concentration of 1.5 mg/mL). Lipid solution was combined with glycerol (Fisher Scientific, Pittsburgh, PA) and Pluronic F-68 (Sigma Aldrich Corporation, St. Louis, MO) in a 1:1:1 mL volumetric ratio. Liquid perfluoropentane (FluoroMed, Round Rock, Texas) was utilized as the dispersed phase.

Microfluidic Device Fabrication

The process for developing the microfluidic wafer has been previously described by Hettiarachchi *et al.*[20] Briefly, microfluidic channels were designed using Illustrator (Adobe, San Jose, CA) and printed at 20,000 dpi by CAD/Art Services (Brandon, OR). In a class 10,000 clean room, a silicon wafer was spin-coated with a UV-curable epoxy (SU-8-25, Micro-Chem, Newton, MA) and exposed to UV light to develop the channels as a negative mold. Bulk polydimethylsiloxane (PDMS) (Dow Corning, Midland, MI) and a curing agent were cast over the wafer at a 10:1 ratio, and the mold was cured at 60°C for at least 8 h. Microfluidic chips were separated from the wafer and cleaned along with the glass slides (2947-75 × 25, Corning, Corning, NY) in a plasma cleaner (Harrick Plasma, Ithaca, NY). The device components were exposed to a plasma field under a controlled pressure of 500 mTorr for 3 min. Upon removal, the microfluidic channels and glass slide were joined, creating a sealed microfluidic device. Then the channels were filled with deionized water to stabilize the hydrophilic environment.

Optical Observations

The microfluidic device was secured to a moving stand on an inverted microscope (Olympus 1 × 71 microscope, Center Valley, PA) with a 50X NA = 1.0 objective. A high-speed camera (Fastcam APX-RS, Photron, Inc., San Diego, CA) was used to capture images and videos of the device output.

Pressure Control Flow System

The reagent pump system was established in a similar manner to Korczyk *et al.*[16] The pressure to control the flow system was supplied by a compressed nitrogen tank connected in parallel to two precision pressure regulators that were used to control the pressure to each reagent independently. A 60 max psi regulator was used to control the continuous phase, and a 30 max psi regulator was used for the dispersed phase (R-800-60 and R-800-30, Air-Trol

Components, Inc., New Berlin, WI). The output of each regulator was connected via Tygon S-54-HL tubing (Saint-Gobain Performance Plastics, Akron, OH) to provide the pressure head to the headspace of a sealed and capped 3 mL glass vial (Figure 1a). Another length of tubing submerged in the reagent (typically 2 mL total) supplied the pressurized fluid to the microfluidic device. By placing a positive pressure head in the vial, the reagent was transferred to the channels of the microfluidic device, and the output rate controlled by manually adjusting the pressure regulators. The system was allowed to stabilize for 1 minute after pressure changes were made before sample collection began.

Optical Imaging and Sizing

Dimensions of the final microfluidic device were determined using Image J (NIH, Bethesda, MD) and a calibrated slide reticule (Edmund Optics, Barrington NJ). The orifice, PFP channel, and lipid solution channel, and filter spacing widths measured 12 μm, 46 μm, 45 μm, and 23 μm, respectively. For micron-sized droplets, diameter was likewise determined optically. Sub-micron droplets could not be resolved optically, and were instead collected in a pipette tip for light scattering or electron microscopy analysis.

Dynamic Light Scattering Sizing

A Malvern Nano ZS (Malvern Instruments Ltd., Malvern, Worcestershire, U.K.) was used to determine the size of droplets in the sub-micron diameter range. Sub-micron samples were diluted with 0.5 mL of phosphate buffered saline and placed into a cuvette for testing. Debris less than 100 nm in diameter were assumed to be lipid vesicles.

Transmission Electron Microscopy (TEM) and Sizing

To verify the presence of perfluorocarbon nanodroplets and corroborate the Malvern sizing data, a negative staining procedure was used alongside TEM (Philips Tecnai 120kV, Amsterdam, The Netherlands). The negative staining first consisted of plasma treating the individual TEM grids for 90 seconds. Ten μl of the droplet sample was transferred via pipette onto the TEM grid and allowed to sit for 120 seconds. The TEM grid was dipped in a bath of 1% uranyl acetate for 60 seconds, and allowed to dry prior to TEM imaging.

Acoustic Droplet Vaporization

To verify that the generated droplet samples could be vaporized, a procedure similar to that described in Sheeran *et al.*[19] was utilized. In brief, a 3.2 MHz transducer with a focal length of 3.45 cm was used to activate the droplets in a cellulose tube submerged in a water bath at 37°C. Droplets within the optical focus were subjected to manually-triggered 100-cycle pulses with 1–2 seconds of rest between each trigger. Pressure was increased in steps of approximately 0.15 MPa until the pressure was sufficient to vaporize the majority (approximately 90% or greater) of the droplets in focus.

Acknowledgments

The authors would like to thank Jason Streeter for producing the initial lipid composition and Roger Shih for manufacture of the master wafer. We appreciate the intellectual contributions of Dr. Terry Matsunaga on medical uses and formulation methods for perfluorocarbon droplets. This grant was supported by R01EB008733 and R21EB011704.

References

1. Kripfgans OD, Fowlkes JB, Miller DL, Eldevik OP, Carson PL. Ultrasound Med Biol. 2000; 26:1177–1189. [PubMed: 11053753]
2. O'Neill BE, Rapoport N. Ther Deliv. 2011; 2:1165–1187. [PubMed: 22059114]

3. Sheeran PS, Dayton PA. Curr Pharm Des. 2012 In Press.
4. Campbell RB. Anticancer Agents Med Chem. 2006; 6:503–512. [PubMed: 17100555]
5. Kawabata K, Sugita N, Yoshikawa H, Azuma T, Umemura S. Jpn J Appl Phys. 2005; 44:4548–4552.
6. Mohan P, Rapoport N. Mol Pharm. 2010; 7:1959–1973. [PubMed: 20957997]
7. Martz TD, Sheeran PS, Bardin D, Lee AP, Dayton PA. Ultrasound Med Biol. 2011; 37:1952–1957. [PubMed: 21963036]
8. Kripfgans OD, Fabiilli ML, Carson PL, Fowlkes JB. J Acoust Soc Am. 2004; 116:272–281. [PubMed: 15295987]
9. Nisisako T, Torii T, Higuchi T. Lab Chip. 2002; 2:24–26. [PubMed: 15100856]
10. Tan YC, Fisher JS, Lee AI, Cristini V, Lee AP. Lab Chip. 2004; 4:292–298. [PubMed: 15269794]
11. Tan YC, Lee AP. Lab Chip. 2005; 5:1178–1183. [PubMed: 16175277]
12. Tan YC, Cristini V, Lee AP. Sens Actuators, B. 2006; 114:350–356.
13. Anna SL, Mayer HC. Phys Fluids. 2006; 18:121512.
14. Cubaud TC, Mason TG. Phys Fluids. 2008; 20:053302.
15. Bardin D, Martz TD, Sheeran PS, Shih R, Dayton PA, Lee AP. Lab Chip. 2011; 11:3990–3998. [PubMed: 22011845]
16. Korczyk PM, Cybulski O, Makulska S, Garstecki P. Lab Chip. 2010; 11:173–175. [PubMed: 20949204]
17. Thorsen T, Roberts RW, Arnold FH, Quake SR. Phys Rev Lett. 2001; 86:4163–4166. [PubMed: 11328121]
18. Ward T, Faivre M, Stone HA. Langmuir. 2010; 26:9233–9239. [PubMed: 20334409]
19. Sheeran PS, Wong VP, Luois S, McFarland RJ, Ross WD, Feingold S, Matsunaga TO, Dayton PA. Ultrasound Med Biol. 2011; 37:1518–1530. [PubMed: 21775049]
20. Hettiarachchi K, Zhang S, Feingold S, Lee AP, Dayton PA. Biotechnol Prog. 2009; 25:938–945. [PubMed: 19455647]

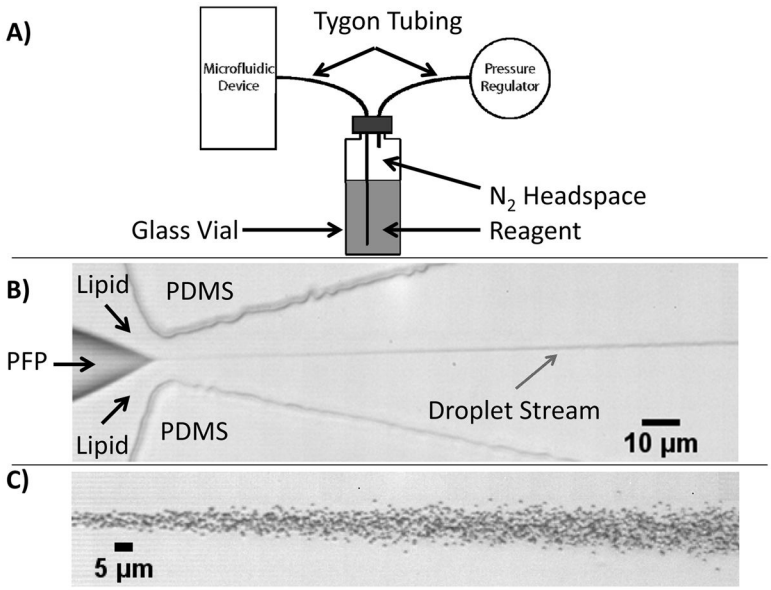

Figure 1.

A) Diagram of pressure-controlled reagent flow, achieved via compressed N_2 driving the reagent through tubing to microfluidic inputs. B) Microscopy of flow-focusing orifice illustrating tip-streaming, resulting in the generation of sub-micrometer droplets. Perfluoropentane (center channel) is surrounded by lipid solution (outer channels). Arrows indicate direction of flow. C) Microscopy of droplets on the order of 800 nm in diameter (larger than shown in the example in (B)) taken downstream of the orifice as the droplet stream widens, illustrating very small, uniform-size production.

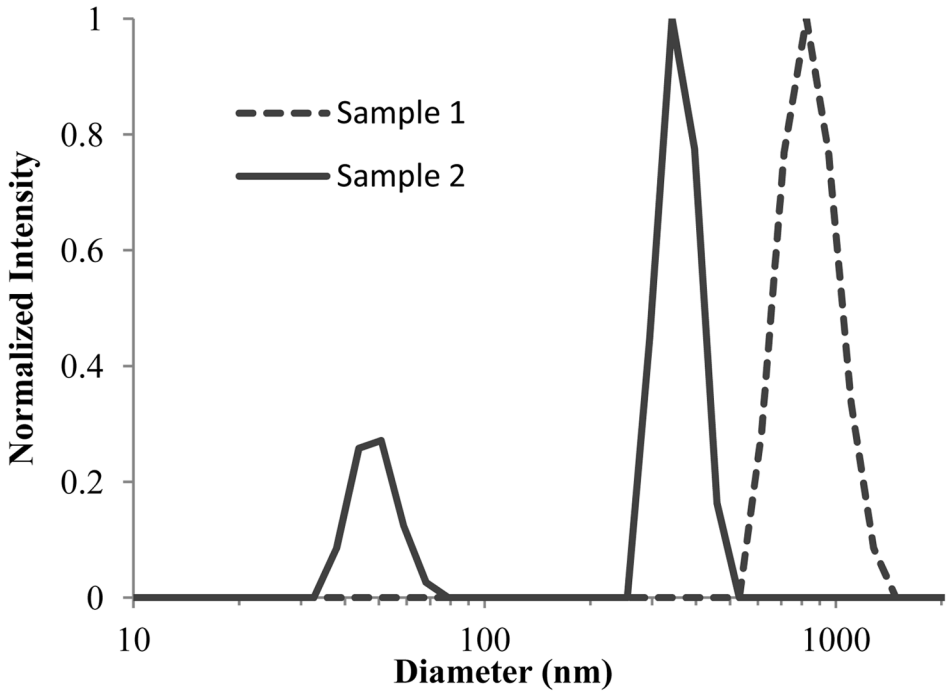

Figure 2.

Particle size distribution produced by DLS for different sub-micron samples produced by the same microfluidic device at different driving pressures. Sample 1 had a mean diameter of 850 ± 150 nm, while Sample 2 had a mean diameter of 360 ± 50 nm in the main peak. Also present in the measurement for Sample 2 are naturally-forming lipid vesicles less than 100 nm in diameter (confirmed by TEM images). For this sample, the lipid vesicles had a mean diameter of 49 ± 7 nm. Each plot is an average of 3 repeat data sets.

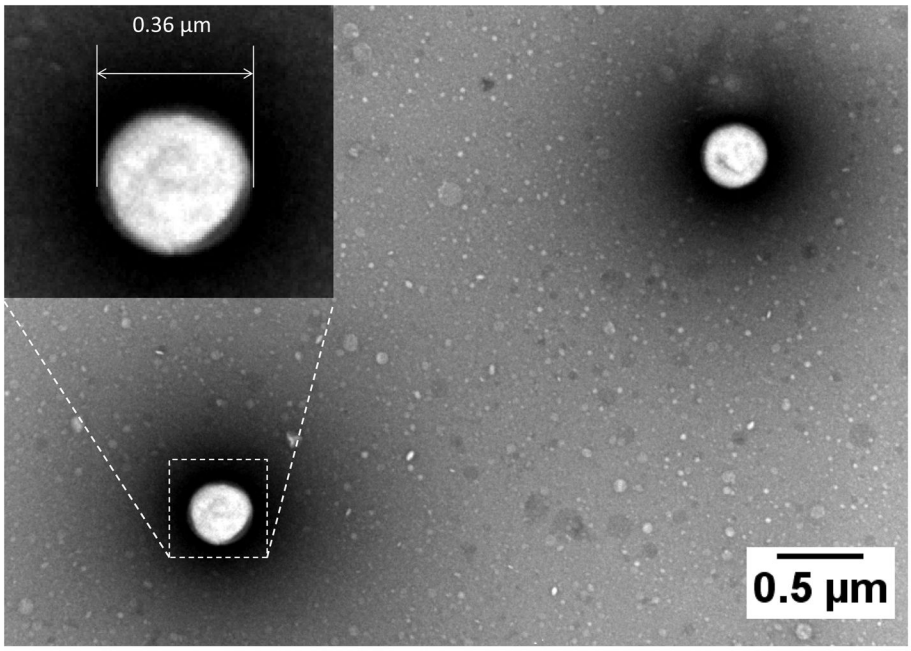

Figure 3.
Transmission electron microscopy example of negative-stained sub-micron perfluorocarbon droplets. The highly-stained droplet circumference appears as a black ring around the droplet core. Lipid vesicles present in the continuous phase can be seen in the TEM image background as semi-circular particles with diameters less than 100 nm, present in high quantities – in agreement with DLS measurements.

Table 1

Droplet Production Characteristics for Various Samples.

Mean Diam. (μm)	Standard Deviation (μm)	Production Rate (droplets/sec)	Input Pressure (psi)†: Continuous Phase	Input Pressure (psi)†: Dispersed Phase
0.36	0.05	*	50	19–20
0.85	0.15	*	44–45	16–17
3.6	0.2	8.7×10^4	33–35	12–15
6.8	0.2	4.0×10^4		
11.7	0.3	3.2×10^4		

* indicates rate is below optical resolution

† range represents observed variation between devices